Temperature-dependent phagocytosis of highly branched poly(*N*-isopropyl acrylamide-*co*-1,2 propandiol-3-methacrylate)s prepared by RAFT polymerization†

Sally Hopkins,[ab] Steven Carter,[a] Linda Swanson,[a] Sheila MacNeil[b] and Stephen Rimmer*[a]

Received 4th June 2007, Accepted 30th July 2007
First published as an Advance Article on the web 16th August 2007
DOI: 10.1039/b708415c

Highly branched poly(*N*-isopropyl acrylamide-*co*-1,2 propandiol-3-methacrylate)s with imidazole end groups and containing anthramethyl methacrylate (AMMA) were prepared. The branch points were produced by incorporating a styryl dithioate ester (a RAFT monomer). The inclusion of AMMA ensures that the polymers fluoresce in the blue region so that they can be visualized in cells in culture. The feed composition was designed to provide lower critical solution temperatures (LCST) between 30 and 37 °C, and therefore the polymers are above the LCST at the usual temperature for culture of human cells. Inclusion of 1,2 propandiol-3-methacrylate (GMA) results in the formation of stable aggregates above the LCST rather than flocculated masses of polymer, and these colloidally stable sub-micron particles can undergo phagocytosis into human dermal fibroblasts. The phagocytosis is temperature dependant and does not occur below the LCST (at 30 °C) when the polymers are in the open-chain fully solvated and non-aggregated state.

Introduction

Poly(*N*-isopropyl acrylamide) (PNIPAM) is a well studied material, which in aqueous solution undergoes a transition from a fully solvated random-coil state to a chain-collapsed non-solvated globule at a lower critical solution temperature.[1] The utility of this material in bioengineering[2] is derived from the temperature range of this transition; typically approximately 32° for the linear homopolymer. The temperature of the LCST makes PNIPAM and its many derivatives useful in a range of biotechnological and medical applications: for example, Galeav *et al.* used imidazole-functionalized linear polymers for temperature-responsive protein-purification procedures,[3–7] and we recently extended this work to the use of highly branched polymers for the purification of a temperature-sensitive recombinant protein implicated in breast cancer.[8,9] The main use of PNIPAM materials in cell biology has been as a temperature-responsive substrate for the culture of mammalian cells.[10,11]

Particulate forms of PNIPAM have potential to deliver drugs in a temperature-controlled manner because the LCST in a microgel causes a step change in the degree of swelling, which induces a change in diffusion characteristics.[12] Several forms of particulate PNIPAM have been reported including core–shell particles[13–15] and microgels.[16–18] However, only a small number of non-cross-linked particulate systems, which are mainly based on block[19,20] or graft copolymers,[21] have been studied. Non-cross-linked particles formed above the LCST progress from an aggregated particulate state to a fully dissolved state as the temperature is lowered. Recently, we considered that highly branched PNIPAM should form stable dispersions above the LCST if the end groups were polar and could provide electrostatic stability to the aggregates.[22] However, we have also observed stable polymer colloids being formed from highly branched *co*-PNIPAM containing also a hydrophilic comonomer (1,2-propandiol-3-methacrylate (GMA)) but with hydrophobic end groups (imidazole end groups in this case). Similar stable dispersions have only very recently been observed.[23,24] As far as we are aware the only reported use of these aggregated particles for entry into human cells involves the use of a random linear copolymer with folate and cholesterol functionality[25] and PNIPAM with DNA binding functionality.[26] Here we report the preparation of fluorescent sub-micron (nano) particles formed from highly branched PNIPAM copolymers, and we show how they can be used for temperature-controlled entry into human cells.

Experimental

Synthesis of fluorescent highly branched stimulus-responsive poly[*N*-isopropyl acrylamide-*stat*-(1,2-propandiol-3-methacrylate)]s (Im28 and Im33)

Im28. NIPAM (1 g, 8.838 mmol, Aldrich 97%, recrystallized from hexane) and 4-vinylbenzylimidazole dithioate[27] (0.0694 g, 0.266 mmol) were dissolved in dioxane (6.0 ml). GMA (0.0688 g, 0.43 mmol) was dissolved in dioxane (1.0 ml). Both solutions were combined and 9-anthryl methyl methacrylate (AMMA) (26.3 mg, 0.0935 mmol) and the initiator α-azo-bis(isobutyronitrile) (AIBN) (0.0438 g) were added. The solution was transferred by syringe to a glass ampoule and freeze pump thaw degassed three times. The ampoule was

[a]*Polymer and Biomaterials Chemistry Laboratories, Department of Chemistry, University of Sheffield, Sheffield, South Yorkshire, UK S3 7HF. E-mail: s.rimmer@sheffield.ac.uk*
[b]*Department of Engineering Materials, The Kroto Research Institute, University of Sheffield, Broad Lane, Sheffield, South Yorkshire, UK S3 7HQ. E-mail: s.macneil@sheffield.ac.uk*
† This paper is part of a *Journal of Materials Chemistry* theme issue on biomedical materials. Guest editor: Cameron Alexander.

sealed and then heated at 60 °C for 48 hours. ^{1}H NMR: ($CDCl_3$, *ca.* 5% CD_3, rt, 250 MHz): δ/ppm 0.7–2.4 (m, NIPAM CH_3, NIPAM CH_2, NIPAM CH, GMA CH_2, GMA CH), 3.6–4.1 (br s, NIPAM NH–C*H*), 6.5–7.1 (CH aromatic), 7.5–7.8 (s, N–CH imidazole)

Im33. NIPAM (1 g, 8.838 mmol) and 4-vinylbenzylimidazole dithioate (0.0818 g, 0.314 mmol) were dissolved in dioxane (6.0 ml). GMA (0.0688 g, 0.43 mmol) was dissolved in dioxane (1.0 ml). Both solutions were combined and AMMA (26.5 mg, 0.0958 mmol) and the initiator AIBN (0.0516 g) were added. The solution was transferred by syringe to a glass ampoule and freeze pump thaw degassed three times. The ampoule was sealed and then heated at 60 °C for 48 hours. ^{1}H NMR: ($CDCl_3$, *ca.* 5% CD_3, rt, 250 MHz): δ/ppm 0.8–2.5 (m, NIPAM CH_3, NIPAM CH_2, NIPAM CH, GMA CH_2, GMA CH), 3.3–4.1 (br s, NIPAM NH–C*H*), 6.5–7.1 (CH aromatic), 7.6–7.8 (s, N–CH imidazole).

Purification

The polymer solution was precipitated by dropwise addition to diethyl ether (200 ml). The diethyl ether was decanted off, the solids were further washed with ether and then vacuum oven dried at room temperature (16 h). This was repeated twice by dissolving in a minimum volume of DMF and precipitating in diethyl ether. Ultra filtration was used to purify the polymer further. A stock solution of 10% ethanol–acetone was made and the ultra filtration equipment rinsed out with water–ethanol. A 10 000 molecular weight cut off cellulose filter was used. The polymer was dissolved in 250 ml of 10% ethanol–acetone and placed in the beaker of the ultra filtration equipment. The solution was stirred, nitrogen gas turned on and the polymer solution filtered until 50 ml remained. 200 ml of stock solution was then added. The procedure was repeated three times. Any remaining solvent was removed by rotary evaporation and the polymer placed in a vacuum oven. The same method of precipitation and ultrafiltration was completed for both polymers

Characterization

GPC was performed to determine average molecular weights and molecular weight distributions measured relative to poly (ethylene oxide) standards using dimethyl formaldehyde containing 1% ammonium acetate as the eluent. Samples were prepared at a concentration of approximately 2.0 mg cm^{-3} in DMF. The solutions were then run through PL gel (mixed-B/3 × 30 cm + guard) columns (Polymer Laboratories) with a refractive index detector at a flow rate of 1.0 cm^3 min^{-1} at 70 °C. Analysis was performed using Cirrus GPC software. Particle sizing was performed on a Brookhaven ZetaPALS particle size analyser. Measurements were carried out on samples at a concentration of 1 mg cm^{-3} in deionized water. The samples were prepared by dissolving the polymers over ice

Turbidimetry measurements

Cloud-point analysis was performed to estimate the LCST of both polymers using a Cary 3Bio UV-Visible spectrophotometer equipped with a Cary temperature controller. The temperature of the cell holder was controlled with a Varian Cary temperature controller to an accuracy of ±0.1 °C. LCST is the temperature at which the point of inflection of the increase in absorbance occurred upon raising the temperature of the sample. Measurements were obtained using a wavelength of 500 nm and a temperature ramp of 10 to 60 °C. Optical density measurements were carried out on samples at a concentration of 1 mg ml^{-1} in deionized water. Nitrogen gas was blown at the sample cell holders to avoid a build up of condensation.

Examination of uptake of polymer by cultured cells

Normal human dermal fibroblasts (HDF) were isolated from human skin as previously described[28] obtained from patients undergoing elective surgery for breast reduction or abdominoplasty. All patients gave informed consent for skin to be used for research. Cells were cultured in 24 well plates (40 000 cells per well) for 48 hours. The media was then removed and replaced with media containing polymer for periods as indicated. The cells were then washed with PBS three times and fluorescent images were captured using an ImageXpress 5000 A automated cellular imaging and analysis system (Axon Instruments, California, USA).

In order to verify that polymer uptake required live cells, ethanol and buffered formaldehyde were then used to kill cells. A 70% ethanol solution was left on the cells for 10 minutes then replaced with media containing polymer to see whether the polymer was being internalized or attaching to the outer membrane of the cells. After the addition of ethanol, cells would not be able to internalize the polymers but polymer may have attached to the surface. The 24 well plate of cells was placed in the incubator for 72 hours. Cells were then washed with PBS three times. 500 μl of 10% and buffered formaldehyde was added to each well to fix the cells (5 min), which were then washed with PBS three times prior to imaging

To visualize the cytoskeleton 180 μl of phalloidin tetramethyl rhodamine (Sigma, P1951) was added to 3600 μl of PBS (1 : 20) and used to stain the F-actin in the cells red. 150 μl of the stain solution was added to each well for 15 min. The cells were washed with PBS three times and fluorescent images were captured.

Results and discussion

PNIPAM polymers usually precipitate above the LCST once the globules that form at the LCST aggregate. However, at low concentration the globules can form colloidally stable dispersions of nanoparticles.[22–24] On the other hand we have recently shown that stable polymer dispersions can be produced above the LCST by adding polar end groups to the chain ends of highly branched PNIPAM.[22] Another possible alternative strategy for producing stable particles above the LCST is to include water-soluble monomers in the backbone so that the swelling ratio of the globule is increased. Also, in order to visualize the particles within cells we included a luminescent comonomer, anthramethyl methacrylate (AMMA). Two highly branched polymers, which were designed using our previously published data[8] to have LCSTs below 37 °C but

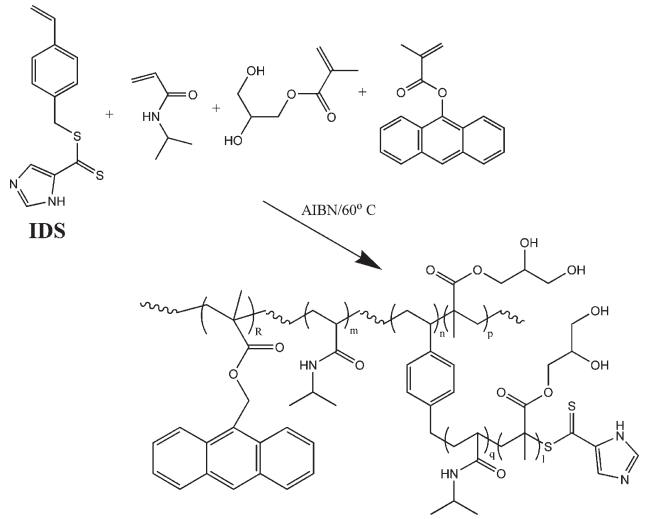

Scheme 1 Synthesis of fluorescent highly branched poly(NIPAM-*co*-GMA) with imidazole end groups.

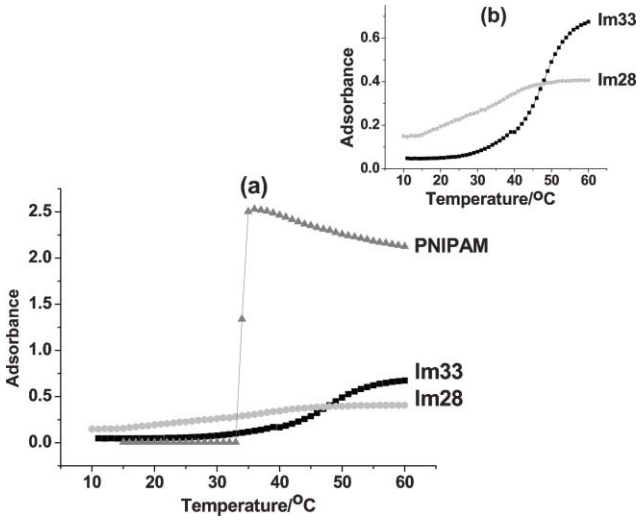

Fig. 2 Turbimetric curves obtained as aqueous solutions of Im33 and Im28 are heated through the LCST.

above the lowest practical temperatures for cell culture, were prepared. As in our previous work the branch points were produced by copolymerization of a styryl dithioate ester, 4-vinylbenzyl-3*H*-imidazole-4-carbodithioate (IDS), with NIPAM. Polymerization monomer feeds contained AMMA and 1,2 propandiol-3 methacrylate (GMA) and provided tetrapolymers with imidazole functionality at the chain ends. The tetrapolymerizations are shown in scheme 1.

Stimulus-responsive highly branched NIPAM tetrapolymers were synthesized by tetrapolymerization of NIPAM, GMA, anthramethyl methacrylate (AMMA) and PDS, using our previously reported method but including AMMA in the monomer feed.[8] The polymers are designated as Im33 and Im28, respectively.

PDS acts as a branching agent since it reacts with propagating radicals at both the dithioester group and the vinyl group, as shown in scheme 1. Control of the polymer composition can be used to control the lower critical solution temperature (LCST), and the presence of the GMA allows the polymers to form stable polymer nanoparticles rather than flocculated masses of polymer. The relative molecular weight distributions derived from SEC are shown in Fig. 1 for Im33 and Im28.

The polymers were ultra filtered during work up to remove low molecular weight molecules below 10 000 g mol^{-1}. Since branching alters the hydrodynamic volume in solution and this is reflected in longer retention times in SEC compared to linear

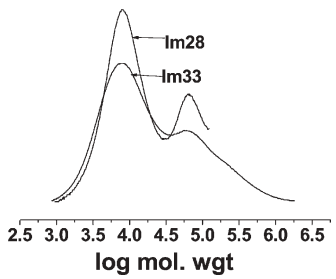

Fig. 1 SEC-derived molecular weight distributions of Im28 and Im33.

analogues, the molecular weight distributions in Fig. 1 should be viewed with some caution. However, not withstanding this comment, the distributions (calculated against polyethylene oxide standards) are clearly broad and multimodal, as expected of this type of polymerization.[27]

In order to estimate the LCST the cloud points were determined by turbidmetry. The turbimetric curves, expressed as readings of adsorbance, are shown for Im33 and Im28 in Fig. 2. Fig. 2(a) illustrates the response of these branched polymers compared to that of linear homo PNIPAM. Clearly, one consequence of the copolymerization and self-condensing vinyl-polymerization processes, and broadening of the molecular weight and composition distributions, was broadening of the temperature range over which the transition occurs. As expected, the cloud point of PNIPAM occurred as a sharp increase in turbidity whereas the response of Im33 and Im28 was more diffuse and occurred over a broad temperature range. One aspect worth noting from these data is that the cloud points of Im33 and Im28 occur as continuous increases in turbidity with no discontinuities. Fig. 2 shows that the transition from solvated polymer to aggregated particle occurs over a larger temperature range for Im28 than for Im33. In this work, we arbitrarily estimate the LCSTs as the mid-points of the inflexion in the turbidity *vs.* temperature curves. The midpoints of these curves for polymer Im33 and Im28 were found to be 37 °C and 35 °C, respectively. Particle sizes of the dispersions were determined at 37 °C. At this temperature, both Im28 and Im33 have particle diameters of approximately 800 nm (Im28 mean diameter = 800 nm ± 15 nm, PDI = 0.23; Im33 = 750 nm ± 25 nm, PDI 0.13)

The polymers include the fluorescent monomer AMMA, which allows us to locate the polymer and determine whether it has been internalized. The hydrophilic monomer, GMA, was included to provide hydrophilic colloidal stability above the LCST. These stimuli-responsive polymers have been synthesized, and the formulation tuned in order to form sub-micron particles when the temperature is above the LCST. The size of these stimulus-responsive particles makes them suitable

candidates for entry into cells and the presence of the fluorescent comonomer should allow us to visualize them inside the cells.

The polymers fluoresce in the blue region allowing us to locate the cells by counter staining F-actin red with phalloidin tetramethyl rhodamine. Fig. 3 shows fluorescent micrographs of human dermal fibroblasts (HDF) that have been incubated at 37 °C in the presence of Im28 and Im33. There is a clear colour contrast between the blue fluorescent polymer particles and the cells' actin cytoskeleton. The fluorescent images are overlaid to show that the polymer corresponds to the position of the cells.

Also Im28 was added at various concentrations, and at each concentration the fluorescent particles appear to be internalized into the cells (as shown in Fig. 4); *i.e.* they occur coincident with the F-actin network.

In order to further confirm the internalization of these particles, which requires the cells to be viable, two different cytotoxic agents were added prior to adding Im28: 70% ethanol and 10% buffered formaldehyde. These were left on the cells for 5 minutes, and after this procedure the polymer was added, in media, to the cells and left for 72 hours. The medium was then changed and the culture plate washed to remove any polymer that had not adhered to the plate or the cells. Fig. 5 shows that the polymer was completely removed from these plates at the washing stage. The cells were still stained with the phaloidin tetramethyl rhodamine stain for the F-actin and visualized but there was clearly no polymer present. Therefore we can conclude that the polymers were not adhering to the cell membrane and they had not been internalized by the dead cells. This suggests that the polymers added to untreated, healthy fibroblasts had been internalized by the cell and are not attached to the cell membrane.

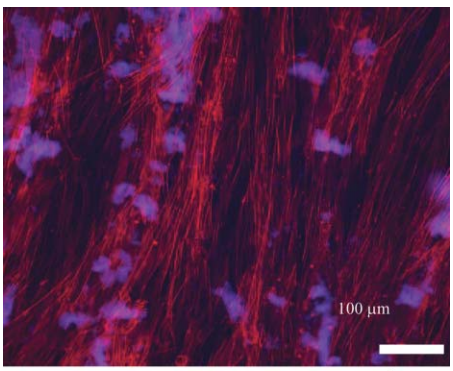

(a) Im28 seeded at 0.625 mg ml^{-1}

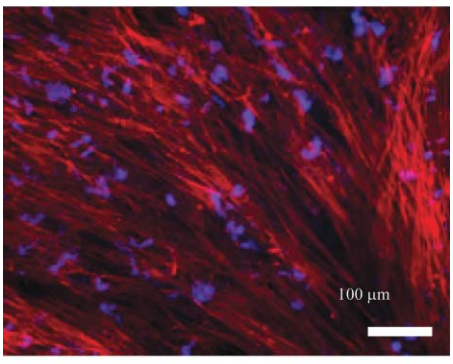

(b) Im33 seeded at 0.625 mg ml^{-1}

Fig. 3 Overlaid fluorescence images of Im28 and Im33 particles internalized in HDFs. Polymer shown in blue F-actin shown in red.

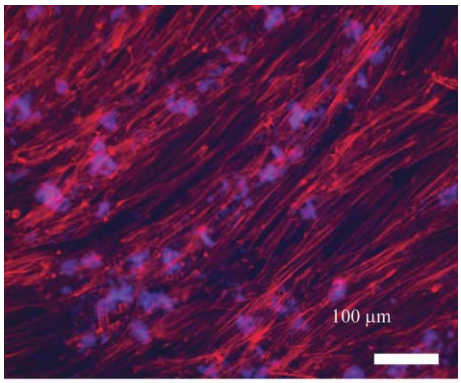

(a) 0.3125 mg ml^{-1}

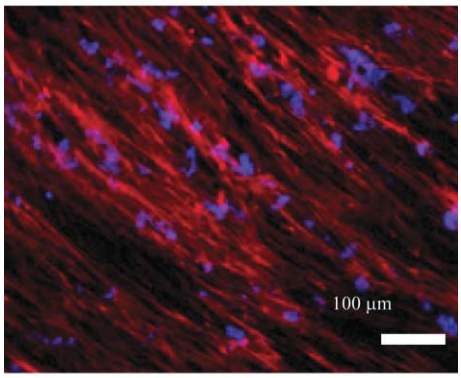

(b) 0.125 mg ml^{-1}

Fig. 4 Micrographs showing the internalization of Im28 in HDFs at two different concentrations. The micrographs show the polymer particles, which fluoresce in the blue region, coincident with the red-stained F-actin cytoskeleton.

It is clear that many formulations and architectures of acrylamide and methacrylate monomers could be produced that would form particles in a size range that would be amenable to cell uptake. For example, commercially available coloured particles produced by emulsion polymerization enter viable cells and are useful for location and visualization. However, the particles described here are unique in that the particles are formed only at physiological temperatures and they are fully soluble below the LCST. Other forms of PNIPAM such as microgels show temperature-responsive swelling but not a transition between the dispersed-particle state and the dissolved state. Since the process of cell uptake is size-dependant, and the transition from a clear solution to a turbid dispersion implies a large increase in size, the opportunity exists to control entry by changes in size driven by changes in temperature. In order to test this hypothesis Im28, which has an LCST of 37 °C, was added to the cell cultures at 37 and 30 °C. However, in order to confirm that the HDFs were capable of cell uptake at 30 °C the experiments were repeated using the commercially available polymer latex particles (Sigma Aldrich, L1398, 2.5% solids, 0.8 μm). Blue-dyed latex beads and Im28 were added to sets of cells and two

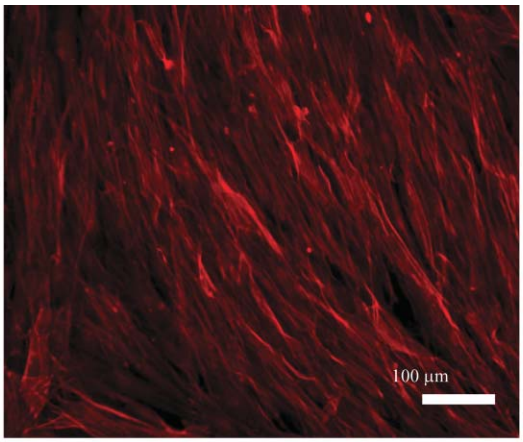

(a) *HDFs treated with 10 % buffered formaldehyde*

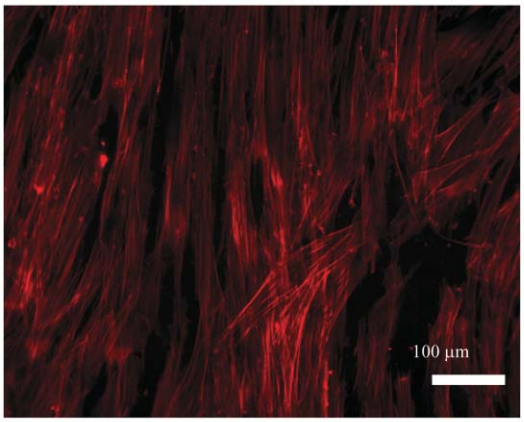

(b) *HDFs treated with 70 % ethanol*

Fig. 5 Micrographs of HDFs after the addition of either ethanol or formaldehyde. Im28 was incubated with these cultures but then removed by washing. Blue colouration, indicative of the polymer is not evident.

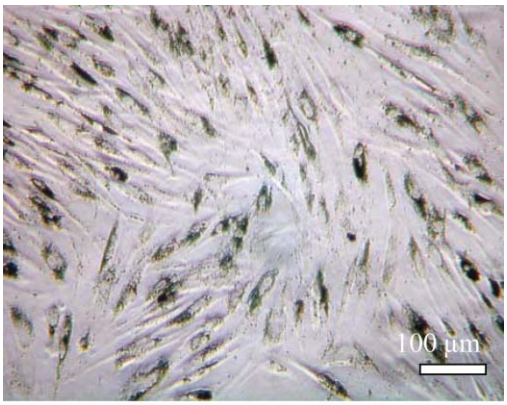

Culture temperature = 37°C

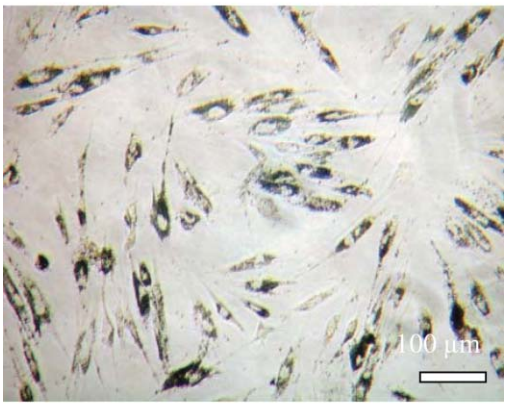

Culture temperature = 30°C

Fig. 6 Micrographs of HDFs cultured at 37 or 30 °C in the presence of blue latex beads. The cells take up the beads at both temperatures.

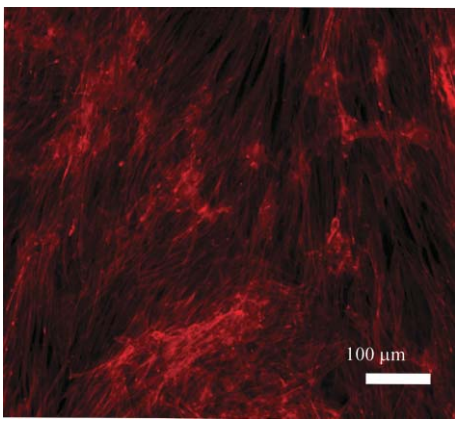

Fig. 7 Micrograph of HDFs exposed to Im28 at 30 °C showing the F-actin network. The blue fluorescent polymer is absent from these cells.

experiments were run in parallel, one at 37 °C and the other at 30 °C. The HDF cells did not become confluent at 30 °C but the polymer beads were internalized into the cells, as shown in Fig. 6.

The micrograph shown in Fig. 7 shows the F-actin network within the cells exposed to Im28 at 30 °C. Clearly, addition of Im28 to the cells at 30 °C does not result in the internalization of the polymer.

Discussion

Dendrimers have been proposed as vectors for the transfection of nucleic acids for a number of years[29–33] and more recently hyperbranched polymers have also been shown to be potentially useful transfection vectors.[34] There are also several technologies that require the entry of small molecule or therapeutic peptides into cells. The entry into cells can be achieved if particles of the correct size can be produced. Typically the particle size of a polymer-delivery particle is set during synthesis or fabrication. However, thermally responsive particles in the form of microgels undergo swelling and deswelling in response to temperature changes, and these phenomena produce changes in particle size but the size changes are confined by the cross-linking network. Here we have introduced new methodology that has some of the features of a stimulus-responsive microgel, in that the primary polymer molecules are composed of branched chains, but the branch points do not result in elastically effective cross-links. The topology of these, highly branched polymers, is essentially

the same as a polymerization reaction mixture containing polyfunctional monomers before the gel point. The advantage of the self-condensing vinyl-polymerization approach used here over other approaches is that the polymerization does not reach a gel point regardless of the composition of the reaction mixture.

The highly branched polymers are fully solvated below the LCST and this study shows they do not enter HDFs. We consider that in this state the polymer chain is highly mobile and the coil size is in the nanometre size range. In previous work we found that highly branched PNIPAM with imidazole end groups precipitated from solution above the LCST to form non-dispersed flocs.[27] These flocs could be used to remove histidine-tagged proteins from solution.[9] However, in this work we added a hydrophilic monomer to the polymerization feed (GMA), which probably produces an increase in swelling above the LCST. As in other PNIPAM systems the polymer chains pass through the coil–globule transition at the LCST. The primary globules then aggregate but, unlike in conventional systems, the aggregates form sub-micron particles that remain stable in aqueous media. From the results shown here it is clear that these particles enter HDFs at 37 °C. The decrease in LCST observed as the degree of branching increases, reported in ref. 27, means that the imidazole groups can be regarded as hydrophobic units that do not contribute to the stability of the particles. These groups are thus available for binding to therapeutics for delivery across the cell membrane. Further work is currently under way on this aspect and will be reported in the near future.

Conclusions

We have shown that aqueous solutions of PNIPAM-based highly branched polymers with imidazole end groups can be formed above the LCST into dispersions of stable sub-micron particles. These dispersions revert to the solution state on cooling and the particles are stabilized by incorporation of a hydrophilic monomer into the monomer feed during a self-condensing RAFT polymerization. Fibroblasts are known to take up many particles, and even coating the surface with non-adhesive species such as poly(ethylene glycol) fails to prevent the uptake of nano-particles.[35] On the other hand these particles enter human dermal fibroblasts above the LCST but the polymers in the solution state (below the LCST) do not enter the cells and they thus offer the potential for temperature-dependant modification.

Evidence that uptake of the particles was dependent on cell-mediated processes rather than any passive mechanism was obtained by demonstrating that uptake required metabolically active cells. Thus, cells treated with ethanol or formaldehyde did not take up PNIPAM particles. These treatments made the cells non-viable but they retained their cell membranes and integrity. Also, uptake was itself temperature-dependent. At 30 °C, cells failed to take up the polymers but they were able to take up the coloured particles, which were used here as a reference material.

References

1 M. Heskins and J. E. Guillet, *J. Macromol. Sci., Pure Appl. Chem.*, 1968, **A2**, 1441.
2 Z. M. O. Rzaev, S. Dinçer and E. Pişkin, *Prog. Polym. Sci.*, 2007, **32**, 534.
3 A. Kumar, I. Y. Galaev and B. Mattiasson, *Biotechnol. Bioeng.*, 1998, **59**, 695.
4 A. Kumar, I. Y. Galaev and B. Mattiasson, *Bioseparation*, 1999, **7**, 185.
5 A. Kumar, I. Y. Galaev and B. Mattiasson, *Bioseparation*, 1998, **7**, 129.
6 A. Kumar, A. A. M. Khalil, I. Y. Galaev and B. Mattiasson, *Enzyme Microb. Technol.*, 2003, **33**, 113.
7 A. Kumar, M. Kamihira, I. Y. Galaev and B. Mattiasson, *Langmuir*, 2003, **19**, 865.
8 S. Carter, S. Rimmer, A. Sturdy and M. Webb, *Macromol. Biosci.*, 2006, **5**, 373.
9 S. Carter, S. Rimmer, R. Rutkaite, L. Swanson, J. P. A. Fairclough, A. Sturdy and M. Webb, *Biomacromolecules*, 2006, **7**, 1124.
10 J. Collett, A. Crawford, P. V. Hatton, M. Geoghegan and S. Rimmer, *J. Roy. Soc. Interface*, 2007, **4**, 117.
11 J. Yang, M. Yamato, C. Kohno, A. Nishimoto, H. Sekine, F. Fukai and T. Okano, *Biomaterials*, 2005, **26**, 6415.
12 S. V. Vinogradov, *Curr. Pharm. Des.*, 2006, **36**, 4703.
13 S. Rimmer, A. N. Mohd. Ramli and S. Lefèvre, *Polymer*, 1996, **37**, 4135.
14 M. Hales, C. Barner-Kowollik, T. P. Davis and M. H. Stenzel, *Langmuir*, 2004, **20**, 10809.
15 Y. Chen, J. E. Gautrot and X. X. Zhu, *Langmuir*, 2007, **23**, 1047.
16 N. Sahiner, W. T. Godbey, G. L. McPherson and T. John, *Colloid Polym. Sci*, 2006, **284**, 1121.
17 S. H. Choi, J. J. Yoon and T. G. Park, *J. Colloid Interface Sci.*, 2002, **251**, 57.
18 Q. Wang, Y. Zhao, Y. Yang, H. Xu and X. Yang, *Colloid Polym. Sci.*, 2007, **285**, 515.
19 J. V. M. Weaver, S. P. Armes and V. Bütün, *Chem. Commun.*, 2002, 2122.
20 Y. You, C. Hong, W. Wang, W. Lu and C. Pan, *Macromolecules*, 2004, **37**, 9761.
21 Y. Zhang, W. Yang, C. Wang, W. Wu and S. Fu, *J. Nanosci. Nanotechnol.*, 2006, **6**, 2896.
22 S. Rimmer, S. Carter, R. Rutkaite, J. W. Haycock and L. Swanson, *Soft Matter*, 2007, **2**, 971.
23 P. Kujawa, F. Tanaka and F. M. Winnik, *Macromolecules*, 2006, **39**, 3048.
24 K. S. Soppimath, C. W. Tan and Y. Y. Yang, *Adv. Mater.*, 2005, **17**, 318.
25 K. S. Soppimath, L.-H. Liu, W. Y. Seow, S.-Q. Liu, R. Powell, P. Chan and Y. Y. Yang, *Adv. Funct. Mater.*, 2007, **17**, 355.
26 B. R. Twaites, C. de las Heras Alarcón, D. Cunliffe, M. Lavigne, S. Pennadam, J. R. Smith, D. C. Górecki and C. Alexander, *J. Controlled Release*, 2004, **97**, 551.
27 S. Carter, B. Hunt and S. Rimmer, *Macromolecules*, 2005, **38**, 4595.
28 M. C. Higham, R. Dawson, M. Szabo, R. Short, D. B. Haddow and S. MacNeil, *Tissue Eng.*, 2003, **9**, 917.
29 N. Ardoin and D. Astruc, *Bull. Soc. Chim. Fr.*, 1995, **132**, 875.
30 A. W. Bosman, H. M. Janssen and E. W. Meijer, *Chem. Rev.*, 1999, **99**, 1665.
31 D. C. Tully and J. M. J. Fréchet, *Chem. Commun.*, 2001, 1229.
32 C. C. Lee, J. A. MacKay, J. M. J. Fréchet and F. Szoka, *Nat. Biotechnol.*, 2005, **23**, 1517.
33 S. Svenson and D. A. Tomalia, *Adv. Drug Delivery Rev.*, 2005, **57**, 2106.
34 C. M. Paleos, D. Tsiourvas and Z. Sideratou, *Mol. Pharmacol.*, 2007, **4**, 169.
35 A. K. Guota and A. S. G. Curtis, *J. Mater. Sci.: Mater. Med.*, 2004, **15**, 493.